Examination of the Exchange Interaction through Micellar Size. 3. Stimulated Nuclear Polarization and Time Resolved Electron Spin Resonance Spectra from the Photolysis of Methyl Deoxybenzoin in Alkyl Sulfate Micelles of Different Sizes

Valery F. Tarasov,[*,†] **Elena G. Bagranskaya,**[‡] **Ilya A. Shkrob,**[§]
Nikolai I. Avdievich,[‡] **Naresh D. Ghatlia,**[⊥,‖] **Nikita N. Lukzen,**[‡]
Nicholas J. Turro,[*,⊥] **and Renad Z. Sagdeev**[‡]

*Contribution from the Department of Chemistry, Columbia University,
New York, New York 10027, Institute of Chemical Physics, Russian Academy of Sciences,
Moscow 117334, Russia, International Tomography Center, Novosibirsk 630090, Russia, and
Chemistry Division, Argonne National Laboratory, Argonne, Illinois 60439*

Received July 1, 1994[⊗]

Abstract: Stimulated nuclear polarization (SNP) and time resolved electron spin resonance (TR ESR) spectra were recorded during the laser flash photolysis of ^{13}C carbonyl labeled α-methyldeoxybenzoin solubilized in a series of alkyl sulfate micelles of different sizes. While the SNP spectra show a decrease in the splitting of the two hyperfine lines with decreasing micelle size, this decrease in hyperfine splitting is not seen in the experimental TR ESR spectra. The qualitatively different variations between the SNP and TR ESR spectra, as a function of micelle size, were interpreted in terms of the stochastic Liouville equation as applied to the model of the microreactor.

Introduction

Distance-dependent interactions between reactive partners have been best studied by imposing specially designed restrictions on the molecular dynamics of the system. Biradicals with different tether lengths connecting the radical centers[1] and radical pairs constrained within cyclodextrins,[2] micelles,[3] zeolites,[4] and liquid crystalline environments[5] exemplify this strategy. Our attention has focused on the spin selective reactions of geminate radical pairs (RPs) initially generated as triplets in micellar environments. We have found that the electron spin exchange (ESE) interaction between uncoupled electrons of the RP is among the most important factors responsible for determining the influence of the micelle size on (a) the probability of geminate reaction,[6] (b) the efficiency of $^{13}C/^{12}C$ isotope separation[7] due to the magnetic isotope effect (MIE), and (c) the magnetic field effect (MFE)[8] on the yield of reaction products formed via the reactions of geminate RPs.

The ESE is a distance-dependent interaction and hence it is useful to conceptualize an effective or "operative" ESE within the spatial confines of a micelle; furthermore, the ESE is conventionally modelled to decrease exponentially with distance and hence, qualitatively, it is apparent that for a given RP the effective or "operative" ESE increases as the micelle size is reduced. This logic is strongly supported by the experimental observations that (1) the splitting of the antiphase structure of the electron spin resonance (ESR) spectra of micellized spin correlated RPs, believed to be a measure of the ESE, increases as the micelle size decreases[9] and (2) the splitting in the stimulated nuclear polarization (SNP) spectra decreases with decreasing micelle size.[8,10] However, the concept of an effective ESE[3b,7,11] has numerous limitations, the most important of which is the neglect of the details of the diffusional motion of the radicals within the micelle.

† Russian Academy of Sciences.
‡ International Tomography Center.
§ Argonne National Laboratory.
⊥ Columbia University.
‖ Present address: Unilever Research U.S.
⊗ Abstract published in *Advance ACS Abstracts*, December 1, 1994.
(1) (a) Maeda, K.; Terazima, M.; Azumi, T.; Tanimoto, Y. *J. Phys. Chem.* **1991**, *95*, 192. (b) Staerk, H.; Busmann, H.-G.; Kuhnle, W.; Treichel, R. *J. Phys. Chem.* **1991**, *95*, 1906. (c) Busmann, H.-G.; Staerk, H.; Weller, A. *J. Chem. Phys.* **1989**, *91*, 4096. (d) Tanimoto, Y.; Takashima, M.; Hasegawa, K.; Itoh, M. *Chem. Phys. Lett.* **1987**, *137*, 330. (e) Bittle, R.; Schulten, K. *Chem. Phys. Lett.* **1987**, *146*, 58. (f) Wang, J.-F.; Doubleday, C., Jr.; Turro, N. J. *Chem. Phys. Lett.* **1988**, *146*, 58. (g) Turro, N. J.; Doubleday, C., Jr.; Hwang, K.-C.; Cheng, C.-C.; Fehlner, J. R. *Tetrahedron Lett.* **1987**, *28*, 2929. (h) Zimmt, M. B.; Doubleday, C., Jr.; Gould, I. R.; Turro, N. J. *J. Am. Chem. Soc.* **1985**, *107*, 6724. (i) Closs, G. L.; Redwine, O. D. *J. Am. Chem. Soc.* **1985**, *107*, 6131. (j) Closs, G. L.; Redwine, O. D. *J. Am. Chem. Soc.* **1985**, *107*, 4433. (k) Closs, G. L.; Miller, R.; Redwine, O. D. In *Chemically Induced Magnetic Polarization*; Muus, L. T.; Atkins, P. W.; McLauchlan, K. A.; Pedersen, J. B., Eds.; D. Reidel: Dordrecht-Holland, 1977. (l) Levin, P. P.; Kuzmin, V. A. *Bull. Acad. Sci. USSR Div. Chem. Sci.* **1988**, *37*, 224. (m) Forbes, M. D. E. *J. Phys. Chem.* **1993**, *97*, 3390. (n) Forbes, M. D. E.; Closs, G. L.; Calle, P.; Gautam, P. *J. Phys. Chem.* **1993**, *97*, 3384.
(2) Lei, X. G. *Res. Chem. Intermed.* **1990**, *14*, 15.
(3) (a) Zimmt, M. B.; Doubleday, C., Jr.; Turro, N. J. *J. Am. Chem. Soc.* **1984**, *106*, 3363. (b) Closs, G. L.; Forbes, M. D. E.; Norris, J. R., Jr. *J. Phys. Chem.* **1987**, *91*, 3592. (c) Shkrob, I. A.; Tarasov, V. F.; Bagrayanskaya, E. G. *Chem. Phys.* **1991**, *153*, 427. (d) Shkrob, I. A.; Tarasov, V. F.; Buchachenko, A. L. *Chem. Phys.* **1991**, *153*, 443. (e) Weller, A.; Staerk, H.; Treichel, R. *Faraday Discuss. Chem. Soc.* **1984**, *78*, 271.
(4) (a) Kaufmann, J. S.; Dybowski, C. *J. Photochem. Photobiol. A* **1990**, *51*, 259. (b) Ramamurthy, V.; Corbin, D. R.; Turro, N. J.; Zhang, Z.; Garcia-Garibay, M. A. *J. Org. Chem.* **1991**, *56*, 255. (c) Garcia-Garibay, M. A.; Zhang, Z.; Turro, N. J. *J. Am. Chem. Soc.* **1991**, *113*, 6212. (d) Turro, N. J.; Zhang, Z. *Tetrahedron Lett.* **1989**, *30*, 3761.
(5) Weiss, R. G.; Treanor, R. L.; Nunez, A. *Pure Appl. Chem.* **1988**, *60*, 999.
(6) Tarasov, V. F.; Ghatlia, N. D.; Buchachenko, A. L.; Turro, N. J. *J. Am. Chem. Soc.* **1992**, *114*, 9517.
(7) Tarasov, V. F.; Shkrob, I. A.; Avdievich, N. I.; Ghatlia, N. D.; Buchachenko, A. L.; Turro, N. J. *J. Am. Chem. Soc.* **1994**, *116*, 2281.
(8) Tarasov, V. F.; Ghatlia, N. D.; Avdievich, N. I.; Turro, N. J. *Z. Phys. Chem.* **1993**, *182*, 227.
(9) Wu, C.-H.; Jenks, W. S.; Koptyug, I. V.; Ghatlia, N. D.; Lipson, M.; Tarasov, V. F.; Turro, N. J. *J. Am. Chem. Soc.* **1993**, *115*, 9583.
(10) Avdievich, N. I.; Bagranskaya, E. G.; Tarasov, V. F.; Sagdeev, R. Z. *Z. Phys. Chem.* **1993**, *182*, 107.
(11) McLauchlan, K. A.; Natras, S. R. *Mol. Phys.* **1988**, *65*, 1483.

Scheme 1. Different Reaction Channels Seen during the Photolysis of α-Methyldeoxybenzoin
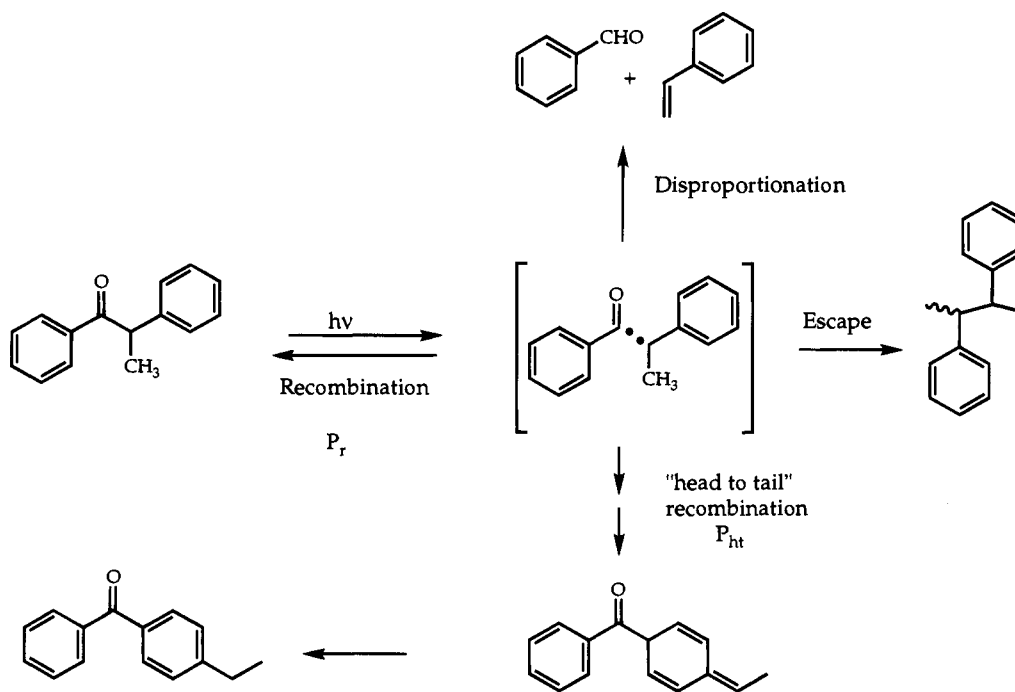
Conceptually, the SNP experiment[12] utilizes the technique of nuclear magnetic resonance to record the ESR spectra of the partners of the RP. However, there is a fundamental distinction between the methods of SNP and ESR: while SNP detects radicals which have undergone a reactive collision just prior to the act of observation, ESR detects those radicals which have avoided reaction prior to the observation. Therefore, the methods follow radicals undergoing different diffusional trajectories. Obtaining information concerning these trajectories was our motivation for comparing the experimental SNP and time resolved (TR) ESR spectra of the geminate RP comprised of the benzoyl and *sec*-phenethyl radicals in alkyl sulfate micelles of different sizes. The latter RP was generated by photolyzing α-methyldeoxybenzoin (MDB). The choice of the radical pair was determined by the fact that the reaction ability,[6,7] magnetic isotope effect (MIE),[3d,7] and magnetic field effect (MFE)[3d,8] of this RP, as a function of micelle size, have already been investigated both experimentally and theoretically. In this work we also report the results from the theoretical simulation of both the TR-ESR and SNP spectra which were calculated using the stochastic Liouville equation[13] as applied to the model of the microreactor.[14]

Another goal of the theoretical fitting of the experimental observations is to discuss the effects of fast geminate chemical reaction in the contact state of the RP on the experimentally observed SNP and ESR spectra of spin correlated RPs. The role of dipole—dipole interaction (DDI) induced relaxation and relaxation due to anisotropic hyperfine interactions (HFI) and their influence on the spectral parameters are examined as well.

Experimental Section

The SNP experimental setup has been reported previously.[12a] The micellar solutions were photolyzed at a repetition rate of 15 Hz by 15 ns pulses of $\lambda = 308$ nm, generated by a Lambda-Physik excimer laser, in the field of a home-made magnet ($B_0 = 0-700$ G) in the resonance microwave field B_1 ($\omega_0 = 310$ or 1530 MHz). The photolyzed solution was transferred into the probe of an NMR spectrometer (Bruker AM-250) with a flow system (transfer time 1—3 s). The longest possible microwave pulse was ca. 30 μs. Since the lifetime of the RP is less than 2 μs these conditions are analogous to continuous-wave pumping. The maximum amplitude of B_1 in a rotating frame was 1.0 mT. The amplitude of the microwave field was estimated from the voltage on the dielectric probe which was placed close to the resonance coil. The values of B_1 were calculated from the known power of the microwave power supply, quality factor of the coil, and the effective volume of the coil.[15]

All ESR spectra were acquired on a Bruker ER100 D X-band ESR spectrometer operated in the direct detection mode with the signal recorded by an EG&G PARC 4402 boxcar and a 4422 integrator. The solutions were flowed through a flat suprasil cell, with an optical path length of 0.5 mm, at the rate of 0.7 mL/min. Excitation was provided either by a Quanta-Ray DCR 2A Nd:YAG laser operating at 266 nm and 20 Hz with 8 ns pulses or a Lambda-Physik excimer laser operating at 308 nm and 5 Hz with 15 ns pulses. In both cases the pulse energy was controlled to be 15 ± 1 mJ/pulse.

^{13}C (99%) carbonyl labeled MDB was prepared from ^{13}C labeled alanine (Cambridge Isotopes Ltd.) using the method of McKenzie et al.[16] Sodium dodecyl sulfate (C_{12}) was obtained from Bio-Rad and used as received. All other detergents [sodium *n*-undecyl sulfate (C_{11}), sodium *n*-decyl sulfate (C_{10}), sodium *n*-nonyl sulfate (C_9), and sodium *n*-octyl sulfate (C_8)] were obtained from Lancaster Synthesis and were purified by recrystallization from ethanol—ether mixtures. The concentration of MDB used was ∼3.3 mM; the concentrations of the detergents used were [C_{12}] = 100 mM, [C_{11}] = 100 mM, [C_{10}] = 120 mM, [C_9] = 130 mM, [C_8] = 200 mM, and [C_7] = 450 mM so as to keep the occupation number approximately constant for different micelles.

All samples were prepared by prolonged stirring of MDB with the detergent solutions and purged with He prior to the measurement.

(12) (a) Sagdeev, R. Z.; Bagryanskaya, E. G. *Pure App. Chem.* **1990**, *62*, 147. (b) Bagryanskaya, E. G.; Grishin, Yn. A.; Sagdeev, R. Z.; Molin, Yu. N. *Chem. Phys. Lett.* **1985**, *114*, 138. (c) Bagryanskaya, E. G.; Grishin, Yn. A.; Sagdeev, R. Z. *Chem. Phys. Lett.* **1985**, *113*, 234. (d) Bagryanskaya, E. G.; Grishin, Yn. A.; Sagdeev, R. Z. *Chem. Phys. Lett.* **1985**, *117*, 220.

(13) (a) Steiner, U. E.; Wolf, J.-H. In *Photochemistry and Photophysics*; Rabek, J. F., Scott, G. W., Eds.; CRC Press: Boca Raton, 1991. (b) Steiner, U. E.; Ulrich, T. *Chem. Rev.* **1989**, *89*, 51. (c) Salikhov, K. M.; Molin, Yu, N.; Sagdeev, R. Z.; Buchachenko, A. L. *Spin Polarization and Magnetic Field Effects in Radical Reactions*; Elsevier: Amsterdam, 1984.

(14) (a) Tarasov, V. F.; Buchachenko, A. L.; Malsev, V. L. *Russ. J. Phys. Chem.* **1981**, *55*, 1921. (b) Sterna, L.; Ronis, D.; Wolfe, S.; Pines, A. *J. Phys. Chem.* **1980**, *73*, 5493.

(15) (a) Mair, L. C.; Slater, J. C. *J. Appl. Phys.* **1952**, *26*, 68. (b) Nakamura, M. *Jpn. J. Appl. Phys.* **1968**, *7*, 173.

(16) McKenzie, A.; Roger, R.; Wills, G. O. *J. Chem. Soc.* **1927**, 779.

112   *J. Am. Chem. Soc., Vol. 117, No. 1, 1995*

Tarasov et al.

Table 1. Values of the Parameters Used in the Calculations (Unless Noted Otherwise)

n for C_n[a]	$10^8 L$ (cm)[b]	$10^6 D$ (cm^2/s)[b]	σ[b]	$10^{12}\tau_c$ (s)[c]
12	15.4	0.79	0.0432	60
11	14.2	1.01	0.0358	49
10	12.9	1.25	0.0292	38
9	11.6	1.49	0.0245	32
8	10.3	1.73	0.0206	27
7	9.0	1.98	0.0169	23

[a] The number of carbon atoms in the detergent chain. [b] The choice of the values used is discussed in refs 6 and 7. [c] The values used for the anisotropic HFI induced paramagnetic relaxation rates.
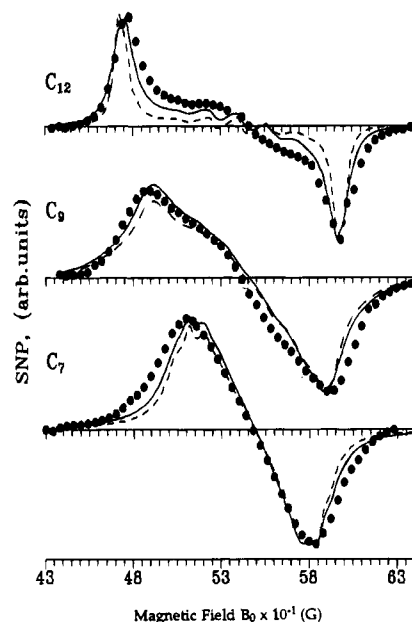
Results

Methyldeoxybenzoin undergoes homolytic α-cleavage[17] upon photoexcitation to generate a RP comprised of benzoyl/*sec*-phenethyl radicals. The RP may (1) recombine to regenerate substrate, (2) disproportionate to produce styrene and benzaldehyde, (3) recombine in a head-to-tail fashion followed by a H shift to give *p*-ethylbenzophenone, or (4) escape into the bulk aqueous phase from the micelle interior (Scheme 1). It is important to note that the reactions 1−3 have been shown to occur only within the micelle interior.[6,7]

There exists a linear relationship[18] between the number of carbon atoms in the hydrocarbon tail of the detergent molecule and the micellar size (measured as some effective value). These values, as estimated by Tanford,[18] are given in Table 1[6,7] and should be considered as characteristic values only. The other important micellar parameter that is relevant to our study is the viscosity of the micellar phase (η) and the rate of radical escape (k_e). The values of the coefficients of mutual diffusion (D) of the RP partners and the boundary factors (σ, vide infra) are also presented in Table 1.

SNP High Field. Figure 1 shows the SNP spectra recorded during the photolysis of MDB in C_{12} (Figure 1a), C_9 (Figure 1b), and C_7 (Figure 1c) micelles in an external field of $B_0 = 550$ G. These spectra were acquired for the ^{13}C NMR resonance of the 99% isotopically enriched carbonyl carbon of MDB. The spectra consist of two lines of different sign (A/E = absorbtive/emissive) and are consistent with a triplet born geminate RP.[19] The distance between the two extrema represents an experimental parameter referred to as $\Delta\omega_0$. In large micelles (C_{12}) this value equals the HFI constant of the corresponding ^{13}C nuclear in the benzoyl radical: $\Delta\omega_0 = A(^{13}\text{C}) \approx 125$ G.[20] This equality is in agreement with the theoretical prediction for high-field SNP acquired under the condition that $B_1 \ll A$ and that ESE is negligible. The ^{13}C SNP spectra acquired on the carbonyls of the other products of the reaction (benzaldehyde and *p*-ethylbenzophenone) are the same as that seen for MDB; this similarity is indirect evidence for the suggestion that the branching of the geminate RP reaction into the different reaction channels occurs after the completion of ISC.[6,7]

It can be seen from Figure 1 that $\Delta\omega_0$ decreases as the length of the hydrocarbon tail of the detergent decreases. The values of $\Delta\omega_0$ and the line width $\delta_{1/2}$, which varies with C_n as well, measured at half the maximum intensity of the individual SNP lines are presented in Table 2.

The variation of $\Delta\omega_0$ with C_n may be qualitatively understood as follows: A decrease in C_n leads to a decrease in micelle

(17) (a) Lewis, F. D.; Magyar, J. G. *J. Am. Chem. Soc.* **1973**, *95*, 5973. (b) Heine, H.-G.; Hartmann, W.; Kory, D. R.; Magyar, J. G.; Hoyle, C. E.; McVey, J. K.; Lewis, F. D. *J. Org. Chem.* **1974**, *39*, 691.
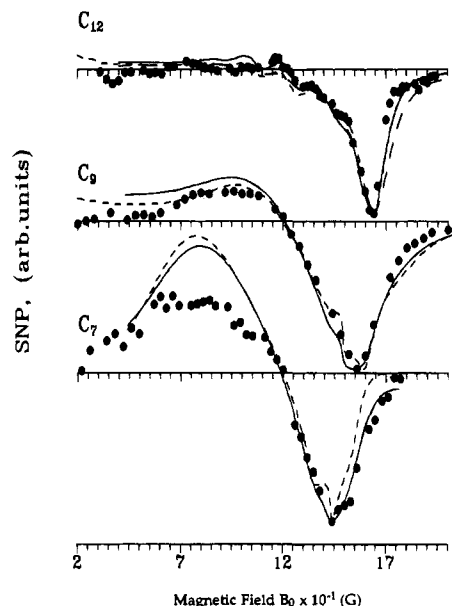
(18) Tanford, C. *J. Phys. Chem.* **1972**, *76*, 3020.

(19) Michailov, S. A.; Salikhov, K. M.; Plato, A. M. *Chem. Phys.* **1987**, *117*, 197.

(20) Landolt-Bornstein. *Organic C Centered Radicals*; Springer: Berlin, 1977; Vol. 1, Part b, p 127.

Figure 1. SNP spectra in alkylsulfate micelles C_n in a high magnetic field (filled circles): (a) $n = 12$, $B_1 = 150$ G; (b) $n = 9$, $B_1 = 300$ G; (c) $n = 7$, $B_1 = 150$ G. Solid lines are simulated spectra in which both anisotropic HFI and DDI induced paramagnetic relaxation have been considered. Dashed lines correspond to simulated spectra in which paramagnetic relaxation has been ignored.

Table 2. Experimental Splitting and Line Widths of the High- and Low-Field Components of the SNP Spectra in Different Micelles

n for C_n	ω_0 (G)	$\delta^+_{1/2}$ (G)[a]	$\delta^-_{1/2}$ (G)[a]
7	74 ± 2	36 ± 2	36 ± 2
8	84 ± 2	53 ± 2	41 ± 2
9	104 ± 2	56 ± 2	44 ± 2
11	120 ± 2	32 ± 2	33 ± 2
12	124 ± 2	23 ± 2	20 ± 2

[a] $\delta^+_{1/2}$ is the line width of the high-field component and $\delta^-_{1/2}$ is the line width of the low-field component.

size[18] and consequently to a decrease in the average distance between the radical centers. This causes an increase in the effective ESE and hence a decrease in the splitting of the lines, since it is known that a strong ESE reduces the observable hyperfine splitting in the ESR spectra for some stable biradicals,[21] and when it is very strong it is half the value of the HFI constant (actually the splitting in the SNP spectra of short-lived biradicals equals $A/2$[22]). However, this simple argument is incomplete since it is based on the concept of an effective ESE, which is only valid in the limit of fast encounters relative to the HFI, i.e. $A/Z \ll 1$ where Z is the frequency of forced encounters of the radical partners.[6,7] It is unlikely that this inequality is fulfilled for the RP under consideration, especially in the larger micelles (C_{12}, C_{11}) where Z is smaller relative to the smaller micelles. Therefore a more rigorous analysis in terms of a detailed computer simulation is required. Another problem which we will try to address is whether the parameters used to simulate the reaction ability of the RP can also be used in the simulation of the SNP and TR ESR spectra.

SNP Spectra, Low Field. The SNP spectra obtained during the photolysis of MDB in a low external field of $B_0 = 124$ G ($\omega_0 = 347$ MHz) in different alkyl sulfate micelles are shown in Figure 2. The disappearance of the low-field component of

(21) Reitz, D. C.; Weissman, S. I. *J. Chem. Phys.* **1960**, *33*, 700.

(22) Koptyug, I. V.; Lukzen, N. N.; Bagryanskaya, E. G.; Docotorov, A. B.; Sagdeev, R. Z. *Chem. Phys.* **1992**, *162*, 53.

Figure 2. SNP spectra in alkylsulfate micelles C_n in a low magnetic field with $B_1 = 300$ G for all cases: (a) $n = 12$, (b) $n = 9$; and (c) $n = 7$. Solid lines are simulated spectra in which both anisotropic HFI and DDI induced paramagnetic relaxation have been considered. Dashed lines correspond to simulated spectra in which paramagnetic relaxation has been ignored. In cases a and d (long dashed curve) the biexponential correlation function was used [$\tau_d = 8 \times 10^{-10}$ s for part a; $\tau_d = 3 \times 10^{-10}$ s for part d].

the spectra in C_{12} and C_{11} micelles is a striking feature as compared to the spectra at high fields (Figure 1) and could be explained by the fact that the strength of the resonance field B_0 equals the value of the HFI constant of the carbonyl carbon in the benzoyl radical. However, the low-field absorbtive component clearly appears in the smaller micelles C_9–C_7 although its intensity is weaker than the emissive component. This effect can be rationalized by a contribution of the ST_- mechanism of the microwave induced nuclear polarization (*vide infra*). Note that, contrary to the prediction of Osintzev et al.,[23] we did not detect any three-line spectra.

Time-Resolved ESR. The TR ESR spectra obtained during the photolysis of ^{13}C labeled MDB in C_{12}, C_{10}, and C_8 micelles are presented in Figures 3, 4, and 5, respectively. The spectra were acquired approximately 100 ns after the laser flash with a gate width of the boxcar of 250 ns. It should be noted that the shape of the spectra were independent of the boxcar gate width and the time delay between the laser pulse and start of acquisition; in addition the spectra were invariant whether light of $\lambda = 308$ or 266 nm was used as the excitation source. The striking difference distinguishing these three spectra is that while the spectrum in C_{12} micelles (Figure 3) is typical for a spin correlated radical pair (each hyperfine line being split in an *E/A* pattern), the spectrum in C_{10} micelles (Figure 4) shows broadening of the internal lines and narrowing of the external ones, and finally, the spectrum in C_8 micelles (Figure 5) shows the standard spectrum for a radical pair polarized by the triplet radical pair mechanism.

The *E/A* antiphase pattern of Figures 3 and 4 is similar to that reported by Closs et al.[3b] for the radical pair derived by the photoreduction of benzophenone in SDS micelles. This pattern was rationalized on the basis of fast ST_0 mixing induced by a relatively strong HFI and a small effective ESE (J_{eff}). The

---

(23) Osintzev, A. M. Ph.D. Thesis, Kazan, 1993.

maximum and minimum of each hyperfine line in Figure 3 are separated by $2J_{eff}$. Thus J_{eff} can at least be measured, in principle, experimentally. Wu et al.[9] have observed that J_{eff} decreases with increasing alkyl chain length of the detergent. Thus, for example, for a RP comprised of benzoyl and ketyl radical fragments $2J_{eff}$ changes from 2.8 G in hexadecyltrimethylammonium bromide micelles to 6.2 G in decyltrimethylammonium bromide micelles. In the case reported here, $2J_{eff} = 9.0 \pm 1.5$ G in C_{12} micelles, but nothing can be said about this parameter in smaller micelles since the qualitative shape of the spectrum changes significantly.

A decrease in the micelle size leads to an increase in the rate constant of radical escape from the micelle as a result of a "decrease in the hydrophobicity" of the micelle with decreasing micelle size. Therefore, it is reasonable to attribute the observed variations in the spectra as resulting from the superposition of different fractions of spin correlated micellized RPs and random pairs formed by escaped radicals. However, the observed dramatic disappearance of the signal of the spin correlated RP with decreasing micelle size is not compatible with the modest decrease in cage effect seen when micelle size decreases.[6,7]

A better approach to explain the spectral variation with micelle size is to suppose that the observed spectrum is, in fact, the superposition of two different mechanisms of electron polarization: polarization generated in spin correlated radical pairs and the usual ST_0 radical pair mechanism. Note that this possibility has been used to simulate the ESR spectra of micellized RPs (see ref 9). In terms of this approach, the variations in the micellar parameters of size and viscosity change the relative contributions of these two mechanisms. However, neither the change in size nor the change in viscosity (Table 1) is large enough to provide for the rapid loss of spin correlation in the small micelles.

That leaves us with the suggestion that the escaped radicals are polarized themselves, because they were once partners in spin correlated radical pairs, and that the polarization pattern of these escaped radicals is identical with that of the ST_0 mechanism polarization. The theory presented below entirely supports this point of view.

Theory

The spin Hamiltonian $H(r)$ of the RP in the rotating frame is given by

$$H(r) = H_a + H_b - J(r)(2S_aS_b - 1/2) \qquad (1)$$

where H_a and H_b are the spin Hamiltonians of the individual radicals. The last term in eq 1 includes the ESE which may be simulated with an exponentially decreasing distance dependence.[13]

$$J(r) = J_0 \exp[-(r - R)/\lambda] \qquad (2)$$

where r is the separation between the radicals, $\lambda = 0.5$ Å is a parameter representing the decrease of the exchange potential, and J_0 is the spin exchange constant at the recombination radius $R = 5$–6 Å;[25] the value of J_0 will be discussed later. The influence of the ESE is well-documented and its manifestations can be seen in different experiments such as the broadening of the SNP lines,[3c] an extra increase of the $B_{1/2}$ parameter in the MARY spectra,[8] the observation of the antiphase TR ESR spectra of spin correlated RPs,[3b,11,24] and the external magnetic
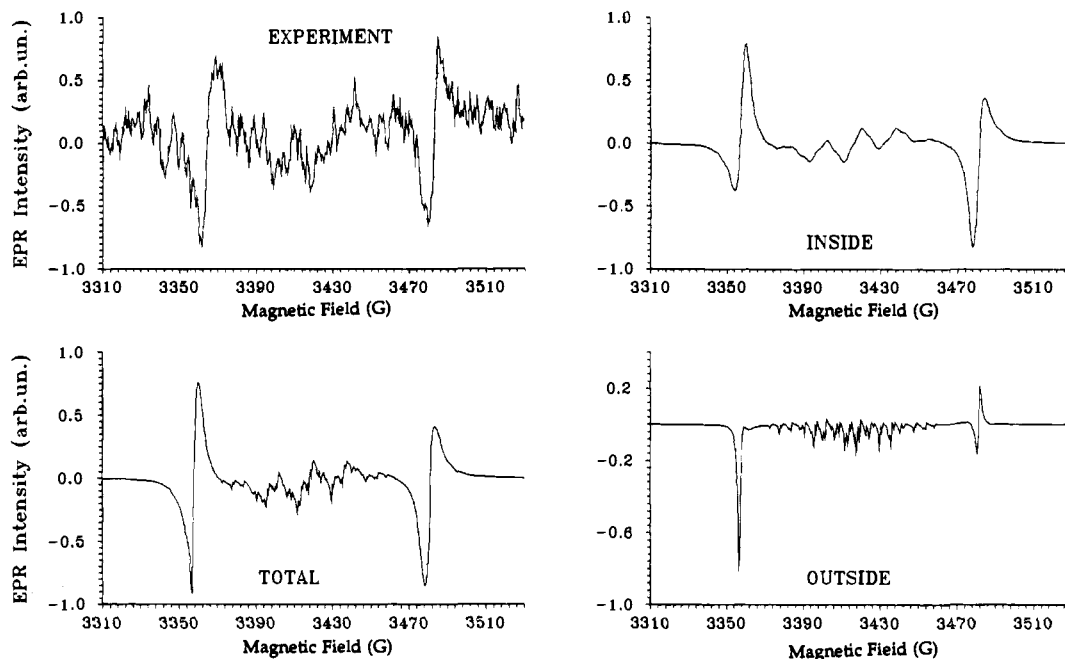
Figure 3. ESR spectra in C_{12} micelles. Spectrum a is the experimental spectrum, and all others are calculated spectra according to the following parameters: $A(^{13}CO) = 124.5$ G; $A(CH_3) = 17.9$ G; $A(CH) = -16.3$ G; $A(H_o) = 4.8$ G; $A(H_p) = 5.9$ G; $B_1 = 10^6$ rad/s; $k_s\tau = 8$; $J_0 = 1.28 \times 10^{10}$ rad/s, $\sigma = 0.0432$; $k_a = k_b = 10^5$ s^{-1}; T_2(benzoyl) $= 8 \times 10^{-8}$ s; T_2(sec-phenethyl) $= 10^{-5}$ s, g(benzoyl) $= 2.0006$, g(sec-phenethyl) $= 2.0026$, $\eta = 0.01$ (see eq 16); all other parameters are presented in Table 1.
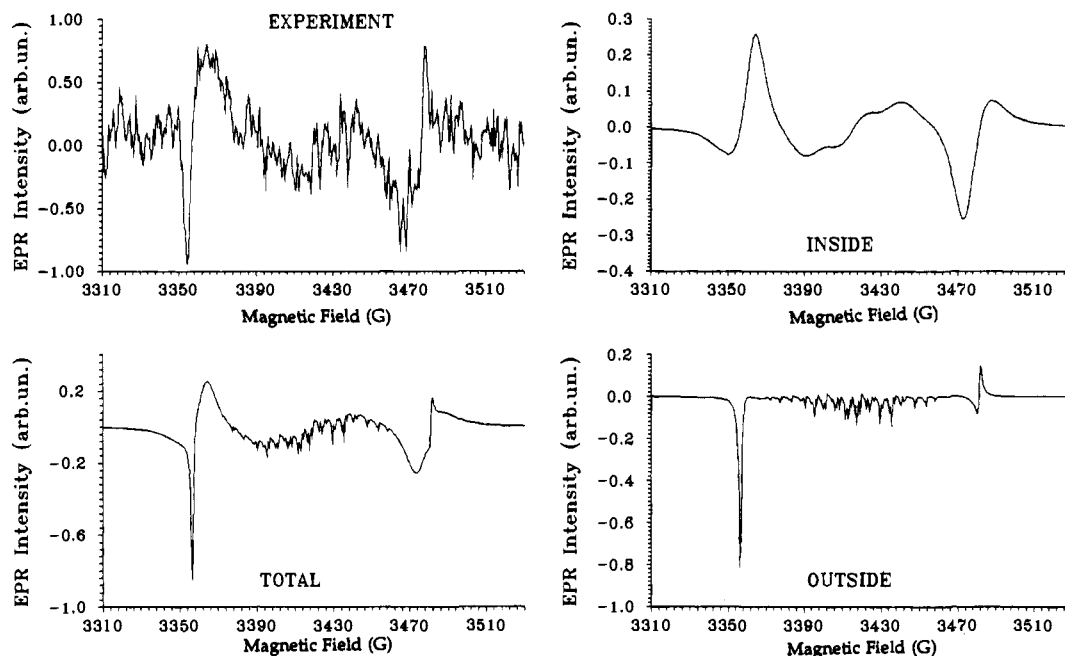
Figure 4. ESR spectra in C_{10} micelles. Spectrum a is the experimental spectrum; all others are calculated with $\tau = 0.0412$, $\eta = 0.008$, and T_2(benzoyl) $= 8 \times 10^{-8}$ s. All other parameters are presented in Table 1 and in the caption for Figure 3.

field dependence of chemically induced dynamic nuclear polarization.[3a]

Hamiltonians H_a and H_b

$$H_\mu = \omega_\mu S_{\mu z} + \omega_1 S_{\mu x}, \quad \text{where } \mu = a, b \tag{3}$$

in eq 1 include the Zeeman interaction of the radicals with the B_0 field and the HFI. In a strong magnetic field:

$$\omega_\mu = g_\mu \mu_B B_0 + \sum_k A_k m_{z,k} - \omega \tag{4}$$

(where g_μ are the g factors of the radicals, μ_B is the electron

Bohr magneton, ω is the microwave frequency, A_k and $m_{z,k}$ are the HFI constant and the spin projection of the kth nucleus, respectively); $\omega_1 = g\mu_B B_1$ is the Rabi frequency.

To calculate the low-field SNP spectra along with eqs 1−4 we also included the nonsecular part of the HFI with the ^{13}C nucleus.

For the sake of simplicity we assume that one of the radicals, say radical a, is located at the center of the micelle while the other, radical b, is free to diffuse within the micellar volume (model of the microreactor[14,3c,d]). This shortcoming of the model is only of relevance during the transient time before the filling out of the micelle; however, since we consider reactions
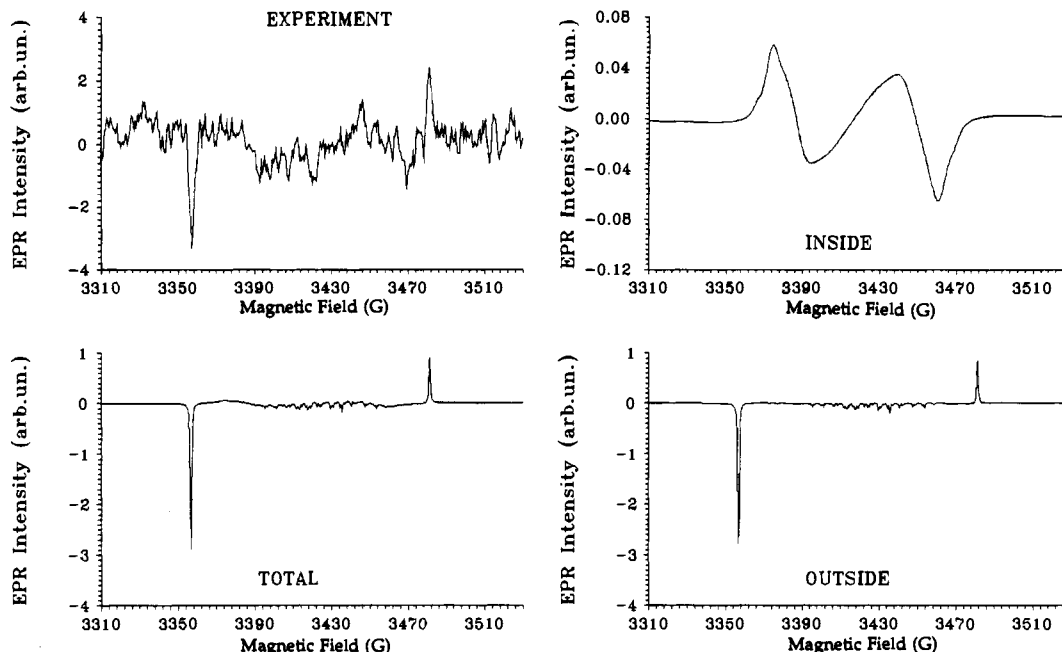
Figure 5. ESR spectra in C_8 micelles. Spectrum a is the experimental spectrum; all others are calculated spectra with $\sigma = 0.0432$, $\eta = 0.01$, and $T_2(\text{benzoyl}) = 2.5 \times 10^{-7}$ s. All other parameters are presented in Table 1 and in the caption for Figure 3.

with characteristic times larger than 100 ns, which are much larger than the filling out time of ~5 ns, we can safely neglect this shortcoming of the model.[6] Radical b may exit the micellar boundary with the rate constant k_{out}. The radicals may also decay with pseudo-first-order rate constants k_a and k_b (to account for side reactions such as scavenging). At a certain distance r = R the pair can recombine through the singlet term with a rate constant k_s. Within the constraints of this model, the escaped radicals never re-enter the same micelle.

This behavior may be described by a system of differential equations

$$d\varrho_{\text{in}}(r)/dt = Dr^{-1} \, d^2(r\varrho_{\text{in}})/dr^2 - L(r)\varrho_{\text{in}}(r) \qquad (5)$$

The index "in" refers to the situation when both radicals are within the micelle. $L(r)$ is the Liouville operator

$$L(r) = -i[H(r)\varrho - \varrho H(r)] + R\varrho + (k_a + k_b)\varrho \qquad (6)$$

where R is the relaxation matrix, which is calculated in the Redfield approach[22] to simulate the SNP spectra. Only the anisotropic HFI with the ^{13}C nucleus is taken into account; we neglect the anisotropic Zeeman interactions because of the relatively small strength of B_0 (<700 G) in the SNP experiment. Later we will compare two approaches for the calculation of the R matrix for the dipole−dipole induced (DDI) paramagnetic relaxation. The first of these approaches is as described by Koptyug et al.[22] and the second is based on Steiner's approximation[24] where translational modulation of the DDI is taken into account. Steiner's approach is described by a biexponential correlation function with the parameters $a_1 = 0.5$, $\tau_1^0 = 0.2$ ns, $a_2 = 0.5$, and $\tau_2^0 = 1$ ns. These are the same values used previously since they have a very weak dependence on the micelle size.

Unlike SNP, TR ESR detects each of the radicals individually: therefore, if one of the radical partners of a pair is scavenged, we are still able to detect the resonance signals from the remaining unreacted radical. This situation cannot be

described correctly when the pair is considered as a single entity, and thus besides the matrix ϱ we should introduce two other matrices ϱ_a and ϱ_b to consider the spin evolution in the individual radicals a and b that are left after the extermination of their partners. Furthermore, there are two possibilities which have to be considered: (1) both observed radicals are inside the micellar core (internal RP) and (2) radical b is outside the micelle (external RP). We assume that the ESE in the external RP equals zero, thus:

$$\varrho(t) = \varrho_{\text{ext}} + \int dr 4\pi r^2 \varrho_{\text{int}}(r,t) \qquad (7)$$

where the subscripts "ext" and "int" stand for the external and internal RPs. Note that the model ignores the situation when both the radicals are outside the micellar core. In addition to eq 7 we should also consider eqs 8, 9, and 10

$$d\varrho_{\text{ext}}/dt = 4\pi L^2 D[d\varrho_{\text{in}}/dr]_{r=L} - L_{\text{ext}}\varrho_{\text{ext}} \qquad (8)$$

$$d\varrho_a/dt = k_b \text{Tr}_b\varrho - L_a\varrho_a \qquad (9)$$

$$d\varrho_b/dt = k_a \text{Tr}_a\varrho - L_b\varrho_b \qquad (10)$$

where $L(r)$ and L_μ are the Liouville operators

$$L(r) = -i[H(r)\varrho - \varrho H(r)] + \{R_a \times 1_b + 1_a \times R_b\}\varrho +$$
$$(k_a + k_b)\varrho \qquad (11)$$

$$L_\mu\varrho_\mu = -i[H_\mu\varrho_\mu - \varrho_\mu H_\mu] + R_\mu\varrho_\mu + k_\mu\varrho_\mu \qquad \mu = a, b \qquad (12)$$

$L_{\text{ext}} = L(r \rightarrow \infty)$. For the calculation of the ESR spectra we use another approach to account for the paramagnetic relaxation. We accept that

$$(j|R_\mu\varrho_\mu|j) = 1/T_{1\mu}\{(j|\varrho_\mu|j) - {}^1\!/_2\text{Tr}\varrho_\mu\} \qquad (13)$$

$$(j|R_\mu\varrho_\mu|j) = 1/T_{2\mu}\{(j|\varrho_\mu|j_\mu), \quad \text{if } j \neq j' \qquad (14)$$

where $T_{1\mu}$ and $T_{2\mu}$ are the corresponding relaxation times.

(24) Steiner, U. E.; Wu, J. R. *Chem. Phys.* **1985**, *98*, 259.
(25) Luders, K.; Salikhov, K. M. *Chem. Phys.* **1985**, *98*, 259.

Equations 13 and 14 are an analog of the well-known Bloch equations.

In eq 8 D is the coefficient of diffusion and L is the radius of the available part of the micelle core (Table 1) for the diffusion motion of radical b. $Tr_{a,b}$ are the trace operators projecting matrix ϱ into smaller matrices ϱ_b and ϱ_a, respectively.

At $t = 0$ for a triplet born RP

$$\varrho_{\text{int}}(r;t=0) = \varrho^0 \delta(r - R)/4\pi r R \qquad (15)$$

and $\varrho_{\text{ext}} = \varrho_\mu = 0$ (μ = a, b).

$$\varrho^0 = {}^1/_3\{(1 + \eta)|T_+)(T_+| + |T_0)(T_0| + (1 - \eta)|T_-)(T_-|\} \qquad (16)$$

where η is the triplet mechanism polarization. Equation 8 must be complemented with two boundary equations of mass balance: at the reaction radius R

$$4\pi r^2 D \, d\varrho_{\text{int}}/dr = 4\pi R^2 \Delta k_s Q_s \varrho_{\text{int}} \qquad (17)$$

where Δ is the thickness of the reaction zone. Q_s in eq 17 may be written in two forms:

$$Q_s\varrho = {}^1/_2\{|S)(S|\varrho + \varrho|S)(S|\} \qquad (18a)$$

and

$$Q_s\varrho = |S)(S|\varrho|S)(S| \qquad (18b)$$

Both projectors describe a reaction of the singlet contact RP with a rate constant k_s. In addition, the projection operator given by eq 18a includes the reactive decay of the mixed ST characters in the density matrix. If the reaction rate is high then the results obtained by these two operators differ even qualitatively.[14b] For example, only models using the Q_s operator as described by eq 18a can account for the halving of the splitting in the SNP spectra of RP in small micelles.

At the micellar border $r = L$

$$-4\pi L^2 \, d\varrho_{\text{int}}/dr = 4\pi L^2 \Delta k_{\text{out}}\varrho_{\text{int}} \qquad (19)$$

We introduce a boundary factor $\sigma = k_{\text{out}}/k_{\text{in}}$,[6,7] where $k_{\text{in}} \approx [\Delta L/D]^{-1}$. At $\sigma = 0$ the boundary is an elastic wall. At $\sigma \gg 1$ each encounter with the wall would result in the irreversible escape of the radicals. Estimates of the parameter σ for the alkyl sulfate micelles give $\sigma \approx 0.05-0.1$.[6,7]

The solution of eqs 18 and 19 is computationally demanding. Fortunately, the radicals do not recombine significantly in the water bulk and it is sufficient to solve the problem for the time integrated $\varrho_{\text{int}}(r) = \int_0^\infty \varrho_{\text{int}}(r,t) \, dt$ in the case of SNP. In the case of TR ESR it is a routine practice that the signal

$$M(t) \propto \text{Tr}\{[S_{ay} + S_{by}]\varrho(t) + S_{ay}\varrho_a(t) + S_{by}\varrho_b(t)\} \qquad (20)$$

is averaged over a certain sampling interval (not less than 50–100 ns). This averaging may be regarded as a convolution of the signal $M(t)$ and a rectangular window function $f(t)$

$$\langle M(t)\rangle = \int dt\, f(t) \int dt'\, M(t - t')(\tau_{\text{sp}})^{-1} \exp(-t'/\tau_{\text{sp}}) \qquad (21)$$

where τ_{sp} is the response time of the spectrometer and $\int dt\, f(t) = 1$.

Equation 21 does not simplify the problem, but for a convenient choice of the $f(t)$ $\langle M(t)\rangle$ may be found without calculating the time-dependent matrix $\varrho(t)$. This is true for a t-exponential gate function $f(t) = t \exp(-t/T)$ where T is the gate width.

We will neglect spin–orbit coupling, which has been invoked to explain the numerical experimental results for biradicals,[1g–j,26] since it only influences the intensity of the spectra but not their shape. Only a few reports which consider the spin rotational interaction—to explain the absence of magnetic field effects in sulfur-containing radicals[27]—have been published. We believe that in the absence of good experimental support for spin rotational interactions in the radicals we are dealing with, it is reasonable to neglect this interaction in our discussion.

Discussion

We first consider the simple qualitative predictions obtained using Shushin's two-site model[28] of the RP with one magnetically active nucleus. In terms of this model the RP may exist in two states I and II in which it spends time τ_1 and Z^{-1}, respectively. In state I the singlet RP can recombine with a rate constant which may be identified with k_s. Consequently τ_1 can be identified with τ_r, or $\tau_1 = \tau_r = \Delta R/D$ (see Theory section) since the time which the system spends in the field of the ESE should approximately equal the time the system spends in the range of possible reaction. Z^{-1} which is the time interval between forced encounters may be estimated as $Z^{-1} \approx L^3/(3RD)$. Thus, $\langle k_s\rangle \approx k_s\tau_1 Z$ can be considered as the averaged reaction rate constant of the singlet RP. In a similar fashion one may define the effective exchange interaction[3d] $J_{\text{eff}} = \langle J\rangle = (1/V)\int dv\, \varrho(r)J(r) = 3J_0\lambda R^2/L^3 = \mu Z$ if $\mu \ll 1$ (μ is the probability of exchange per one forced encounter).

Sushin[28] showed that the positions of the lines in the SNP spectra, reaction yield detected magnetic resonance spectra (RYDMR) and ESR spectra can be described, when neglecting paramagnetic relaxation, by eq 22

$$\omega_\pm = \omega_0 \pm {}^1/_2\{AI_z + J_e + Re[(AI_z)^2 + Z^2(J_e\tau_1 - 2i\omega_e\tau_1)^2]^{1/2} \qquad (22)$$

where

$$J_e = Z \, \text{im}\{(k_s/2 + iJ_0)/(\tau_1^{-1} + k_s/2 + J_0)\} \qquad (23)$$
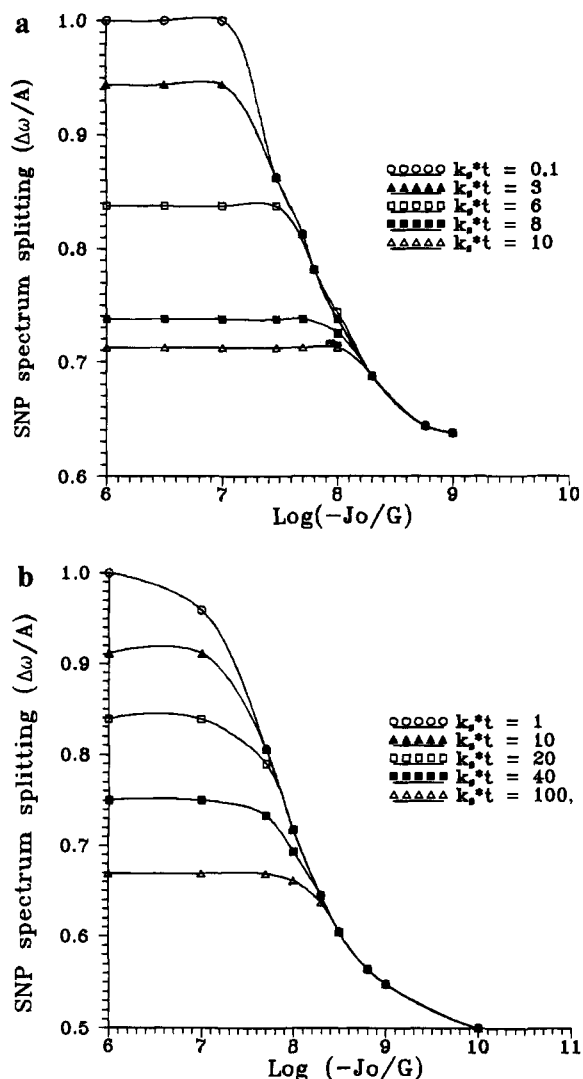
and

$$\omega_e = Z \, \text{Re}\{(k_s/2 + iJ_0)/(\tau_1^{-1} + k_s/2 + J_0)\} \qquad (24)$$

Since $|J_e/Z| < 1$ and $|\omega_e/Z| < 1$ the splitting in the spectrum depends on the ratio A/Z. For the case of $A/Z \gg 1$—the spin mixing does not limit the rate of spin selective reaction—the splitting $\Delta\omega$ equals A irrespective of the values of $k_s\tau_1$ and J_0. In the opposite limit of $A/Z \ll 1$ there are two possibilities. If $Z\tau_1 \ll 2A/(4J_e^2 + k_s^2)^{1/2}$ then the splitting is equal to A and in the other case the splitting is equal to $A/2$. In other words, when ISC is much slower than the reaction rate, both conditions of weak exchange $Z \gg A \gg ZJ_0\tau_1$ and those of slow reaction $Z \gg A \gg Zk_s\tau_1$ should be met for the splitting to remain equal to A. Deviation from any of the equalities leads to $A/2$ line splitting in the ESR or SNP spectra of the spin correlated RPs. Note that the later inequality corresponds to the condition when the rate of radical decay due to spin selective geminate reaction is inversely proportional to the rate of forced encounters.[7] *Thus the halving of the splitting of the ESR or SNP spectra is seen*

(26) Khudyakov, I. V.; Serebrennikov, Y. A.; Turro, N. J. *Chem. Rev.* **1993**, *93*, 537.

(27) Bohne, C.; Alnajjar, M. S.; Griller, D.; Scaiano, J. C. *J. Am. Chem. Soc.* **1991**, *113*, 1444.

(28) Sushin, A. I. *Chem. Phys. Lett.* **1991**, *181*, 274.

Exchange Interaction through Micellar Size

J. Am. Chem. Soc., Vol. 117, No. 1, 1995 117

Figure 6. Correlation between the splitting in the calculated SNP spectra ($\omega_0 = 1530$ MHz) and J_0 and $k_s\tau$ in C_8 micelles: (a) $D = 1.7 \times 10^{-6}$ cm^2/s; (b) $D = 8 \times 10^{-7}$ cm^2/s.

only when ISC limits the rate of reaction and both conditions of strong exchange and fast reaction in the singlet contact state are met.

We now estimate the values of these parameters in our micellar systems. Since D increases (Table 1) from ca. 10^{-6} cm^2/s in C_{12} to 3×10^{-6} cm^2/s in C_7 micelles and L varies from 16 Å in C_{12} to 8 Å in C_7 and $A = 124.5$ G we have A/Z varying from 24 in C_{12} to 1 in C_7 micelles. This variation is sufficient to account for the order of magnitude difference in the critical parameters $Zk_s\tau_1$ and $ZJ_0\tau_1$.

Now let us consider the possible range of variation in the values of J_0 and $k_s\tau_1$. Figure 6a shows the dependence of the splitting in the SNP spectra on J_0 for different values of $k_s\tau_1$ in C_8 micelles. These simulations show that the value of J_0 cannot exceed 10^{10} rad/s and $k_s\tau_1$ must be smaller than $\sim$8. Figure 6b shows the results of the same calculations except that the value of $D = 8 \times 10^{-7}$ cm^2/s; it follows from the data presented in Figure 6b that the upper limit of J_0 is 1.8×10^{11} rad/s. Since $A/Z < 1$ in these low-viscosity conditions the value of $k_s\tau_1$ may be unboundedly large without it being evident in the spectra. Even for $k_s\tau_1 = 100$ the splitting of the calculated spectra is that at $J_0 = 0$:

$$\Delta\omega_0 = A/2 + \text{Re}[(A/2)^2 - Z^2k_s^2\tau_1^2/(1 + k_s\tau_1/2)^2]^{1/2} \quad (25)$$

In the high-viscosity conditions of $A/Z \geq 1$ the variation of $k_s\tau_1$ leads to the variation of the splitting $\Delta\omega_0$ from A ($k_s\tau_1 \ll 1$) to $A/2\{1 + [1 - 4A^2/Z^2]^{1/2}\}$ ($k_s\tau_1 \gg 1$). To fit the experimental results one needs to limit the value of $D \geq 10^{-6}$ cm^2/s, the range of possible values of $J_0 \leq 1.2 \times 10^{10}$ rad/s, and $k_s\tau_1 \leq 12$.

All of the estimates presented above are for the values of L presented in Table 1. It should be noted that there are two arbitrary assumptions used in the model: (1) that one of the radicals is fixed at the center of the micelle and (2) that the escaped radical never reenters the micelle. Both suggestions lead to a decrease in the estimated value of J_0 since the mean distance between the radicals is at least $\sim$1.4 times smaller than the real one (this problem of distance cannot be compensated by the fact that $D = D_a + D_b$).

Figures 1 and 2 shows the calculated SNP spectra in strong and weaker magnetic fields respectively for $k_s\tau_1 = 8$, $J_0 = 1.2 \times 10^{10}$ rad/s and with the values of the parameters presented in Table 1. The values of all the parameters used lie in the range of possible values and were used in the calculation because they have been used[7] to simulate the supercage effect in zero and strong magnetic fields and the dependence of the supercage effect on the micelle size. It can be seen that these parameters can be successfully used to simulate the experimental SNP spectra.

Previous workers[3a] have used the dependence of the line width on the amplitude of the microwave field B_1 to define the value of J_0. In another study,[3c] the value of J_0 was estimated by a comparison of the experimental and calculated MARY spectra. Both of these attempts provided the same value. In the second case, the determined value of J_0 is probably lowered by the fact that HFI with only a limited number of nuclei was considered to approximate the reactivity of the RP in a zero magnetic field. In the first study errors could have arisen due to the neglect of paramagnetic relaxation due to DDI or anisotropic HFI. In this present study, the values of J_0 and $k_s\tau_1$ were defined by the positions of the lines in the SNP spectra. We believe this sort of definition to be more correct, since, as will be shown later, paramagnetic relaxation only leads to a broadening of the lines without any concurrent shift in their positions.

Results obtained from the simulation of the low-field spectra provide additional evidence that the value of J_0 determined by the fitting of the high-field spectra approximates the experimental situation. By monitoring the dependence of the SNP spectra on J_0 in C_8 micelles it is seen that increasing the value of J_0 to 5×10^{10} rad/s leads to an appearance of a low-field absorbtive line in the simulated spectrum, the position and intensity of which is incompatible with the recorded spectrum. Thus the upper limit on the value of J_0 is 5×10^{10} rad/s.

We neglected the paramagnetic relaxation due to anisotropic HFI and DDI in the calculations presented above and have achieved a reasonable agreement with the experimental spectra. Figure 1 shows that incorporating these two relaxation mechanisms in the strong magnetic field allows for a better agreement of the high-field spectra. A more pronounced effect of paramagnetic relaxation is observed in the low magnetic field SNP (Figure 2). Furthermore, the calculated spectra are sensitive to the kind of description of the paramagnetic relaxation due to DDI. It is seen from Figure 2 that Steiner's approach better approximates the experimental results.

The simulated TR ESR spectra are presented in Figures 3–5. The same parameters as used in the calculation of the SNP spectra, with small corrections to the value of boundary factor

118 *J. Am. Chem. Soc., Vol. 117, No. 1, 1995*

Tarasov et al.

σ, were used. However, paramagnetic relaxation was accounted for in a different manner (eq 18).

The successful simulation of the experimental results of both the SNP and ESR techniques allows us to understand the physical nature of the micelle size dependence of the ESR spectra. *First, the dependence of the ESR spectra of the pair inside the micelle shows the same micellar size dependence as do the SNP spectra.* This is not surprising since it is only the internal pair which may react to give a product detected by the SNP method.

Furthermore, the polarization pattern of the external RPs is that of the ST_0 mechanism (Figures 3d, 4d, and 5d). From the theoretical standpoint, this result is due to the non-adiabatic crossing of the boundary by the escaped radical (eq 8). Remember the external RPs do not react according to an assumption of the model, but this assumption is supported by experimental observations.[7] Also, it was assumed that the ESE i the escaped radical is negligibly small. Thus the observed RPM polarization of the external RPs is due to spin coherence transfer. As the exit rate of the radical increases with decreasing micelle size, the relative contribution of the RPM-like pattern due to this transfer becomes large. The loss of the antiphase pattern at longer delay times can be explained not as the loss of spin coherence in the internal RP due to fast relaxation in the radicals but due to the increasing contribution from the escaped RPs polarized through a spin coherence transfer.

The simulated SNP spectra were found to be as sensitive to the value of the boundary factor σ as the ESR spectra. The actual values of σ are unknown; previously, we estimated the dependence of σ on micelle size by analyzing the data on the supercage effect;[7] σ appeared to decrease with micelle size. In the present study we simulated the ESR spectra for C_{12} and C_8 micelles with the same value of $\sigma = 0.04$. We believe that ESR is far more σ sensitive than other spin effect techniques and that the independence of σ on the micellar size is a genuine result. Indeed, the boundary factor must be a property of the radical and the micellar interface rather than the micellar size.

Due to the poor signal-to-noise ratio, we were forced to use a relatively long (250 ns) boxcar integration window and very short delay times (50 ns). These experimental conditions preclude us from discussing the line width of the ESR resonance and therefore not much importance can be placed on the absolute values of $T_{1\mu}$ and $T_{2\mu}$ used in the simulation of the ESR spectra; the values used are presented in the figure captions. Note that the main contributor to the rate of paramagnetic relaxation in the benzoyl radical is the large value of the anisotropic HFI: the inner product of the hyperfine tensor with itself $[A{:}A] \approx 6 \times 10^{16}$ to 1.2×10^{17} rad^2/s^2.[7] The rate of DDI induced paramagnetic relaxation is much slower than that due to anisotropic HFI. To achieve a better agreement with the experimental results we found it necessary to decrease the T_2 times with decreasing micelle size. This is consistent with the experimentally observed shortening of the rotational correlation time when the micelle size decreases.[6]

Conclusions

In this study we have presented results of the SNP and TR ESR investigation of the spin correlated RPs dissolved in alkyl sulfate micelles of different sizes. It was experimentally observed that the splitting between the resonance lines in the SNP spectrum of the geminate radical pair comprising the benzoyl (^{13}C isotope label in the carbonyl group of the radical) and *sec*-phenethyl radicals decreases with micelle size and in the small (C_7) micelles tends to a value of half of the HFI constant. Both the spin exchange and the fast spin selective reaction are responsible for this effect. We also found that unlike the SNP spectra, the ESR spectra do not show the decrease in the splitting between the resonance lines. This apparent discrepancy with the SNP results is explained by the fact that the ESR method detects those radicals which have escaped reaction and therefore as the micelle size decreases the contribution of the radicals which have exited the micelle to the observed spectrum becomes dominant. These escaped radicals are polarized since they have spent some time as a spin correlated RP in the micelle interior and this initial coherence is retained after the radical escapes. The polarization pattern in the escaped radical coincides with that of the ST_0 mechanism.

JA942112U